Bulletin of the Seismological Society of America, Vol. 93, No. 1, pp. 371–385, February 2003

Quantification of Frequency-Dependent Lengthening of Seismic Ground-Motion Duration due to Local Geology: Applications to the Volvi Area (Greece)

by Céline Beauval, Pierre-Yves Bard, Peter Moczo, and Jozef Kristek

Abstract Many methods have been proposed through the last decades for the experimental estimation of site effects. However, these estimates have largely focused on the amplitude of motion, and less attention has been given to duration. The present study is an attempt to fill this gap through a comparison of the phase of the Fourier spectrum at two nearby sites. The method makes use of the frequency-dependent mean group delay as proposed by Sawada (1998). Its application on weak and moderate motion recordings from the European test site near Volvi (Greece) yields stable and physically satisfactory results: the soft sites inside the graben exhibit a consistent increase of the mean group delay, which is maximum around the fundamental frequency of amplification, while rock sites on either side of the graben have comparable spectra, in terms of both modulus and phase. A further comparison with results of 2D finite-difference simulations provides qualitatively similar results. The mean group delays are found, however, to be much smaller on numerical synthetics than on observed records, although the increase of duration for simple input signals is obvious by visual inspection. This may offer a way to discriminate the existence of 2D or 3D effects at a given site. Finally, this technique also allows construction of site-specific time domain synthetics accounting for both the amplitude and phase modifications associated with site conditions. The method requires, however, a good signal-to-noise ratio.

Introduction

Since destructive earthquakes such as the Michoacan earthquake in Mexico (1985), the Northridge, California, earthquake (1994), or the Hyogoken-Nanbu earthquake, Kobe, Japan (1995), there is no more doubt about the importance of site effects during earthquakes in relation to the local geology. Different methods have been developed to estimate site amplification factors from earthquake recordings, but the lengthening of the duration of seismic ground motions has received less attention.

The Volvi test site (Euroseistest, Greece) has already been the source of several instrumental and numeric studies that have revealed the important effects of the graben structure on seismic ground-motion amplitude. Located 25 km northeast of Thessaloniki, this test site aims to create a better understanding of local site effect phenomena for strong ground motion prediction. The Volvi valley is part of the Graben Mygdonian region, a seismically active zone under north-northeast–south-southwest continental extension. The valley trends east–west between the Langhada and the Volvi lakes (Fig. 1) and is filled with alluvial deposits, mainly Quaternary. On the profile where the permanent network stations have been installed, the valley is 5.5 km wide and the sediments are as thick as 200 m in the center. At the northern and southern borders are outcroppings of hard metamorphic rock. The analysis of seismograms shows that the local geology has an influence on the duration of the seismic ground motions: a lengthening of the duration of the signals from the borders to the center of the valley is noted, as displayed in Figure 2. In the present work, we use a method introduced by Sawada (1998) based on signal phase to estimate the arrival time of wave groups. The use of a reference station provides a basis for comparing signal duration as a function of frequency at the different sites.

First we describe the method used for the estimation of ground-motion duration lengthening and test it on synthetic and real signals. Then we apply this method on two different experimental data sets: acceleration signals recorded by the test site permanent network (moderate events, $3.3 \leq M_L \leq 4.6$) and signals obtained on a temporary network ($M_L < 3$) (Riepl, 1997). In the third part, the method is applied to synthetic seismograms based on 2D numeric modeling (Moczo *et al.*, 1996). We finally propose a straightforward

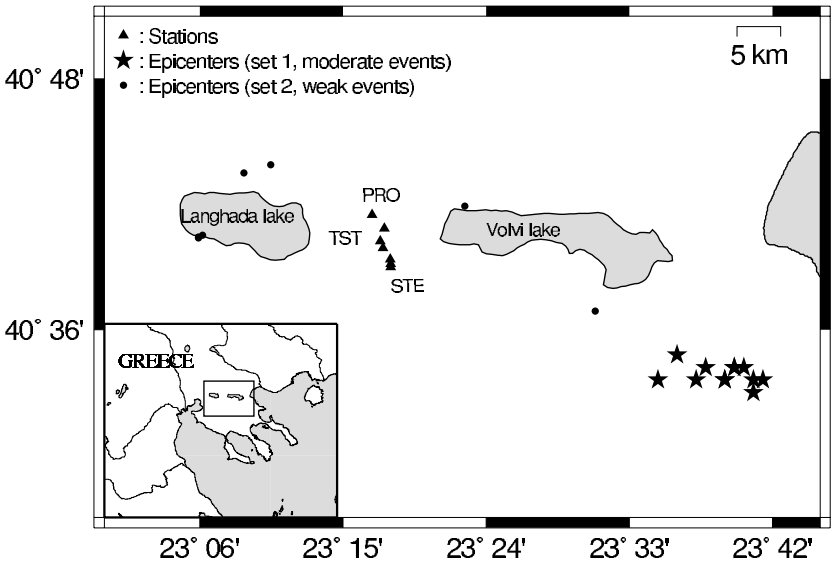

Figure 1. Map of the region where the Euroseistest is installed. Triangles, stations from the permanent network; asterisks, 9 moderate events; circles, 7 weak events. Box in the lower left shows the location map in regional context.

way to generate site-specific synthetic seismograms accounting for the modulus and phase modifications. This approach is particularly relevant in basins and valleys where the 1D numerical approach fails.

Method

Group Delay Time

The method used in this article was proposed by Sawada (1998) to determine the average group delay time of a seismic signal. Taking the Fourier transform $S(\omega)$ of the time history $s(t)$ yields the amplitude spectrum $A(\omega)$ and phase spectrum $\phi(\omega)$:

$$S(\omega) = \frac{1}{2\pi}\int_{-\infty}^{\infty} s(t)\mathrm{e}^{-i\omega t}dt = A(\omega)\mathrm{e}^{-i\phi(\omega)}. \quad (1)$$

The information on signal duration is included in the phase spectrum $\phi(\omega)$. The gradient of the phase contains information on the arrival time of energy as a function of frequency. In order to retrieve this phase gradient, the phase spectrum must be first unwrapped (absolute jumps greater than π are replaced by their 2π complement), then differentiated with respect to frequency, ω. The obtained quantity has a time dimension and is defined as the group delay time (T_{gr}):

$$T_{\mathrm{gr}}(\omega) = \frac{d\phi(\omega)}{d\omega} \quad (2)$$

Because this quantity is very unstable and varies from one frequency to the next (Fig. 3), a smoothing operation is necessary. This is carried out by means of a frequency window function $W(\omega;\omega_0)$ and takes into account the signal amplitude, represented by the Fourier amplitude spectrum $A(\omega)$. As proposed by Sawada (1998), the average spectrum $\mu_{T\mathrm{gr}}(\omega)$ and variance spectrum ${\sigma_{T\mathrm{gr}}}^2(\omega)$ of $T_{\mathrm{gr}}(\omega)$ are defined as follows:

$$\mu_{T\mathrm{gr}}(\omega_0) = \frac{1}{S}\int_0^{\infty} W_A(\omega;\omega_0)T_{\mathrm{gr}}(\omega)d\omega, \quad (3)$$

$${\sigma_{T\mathrm{gr}}}^2(\omega_0) = \frac{1}{S}\int_0^{\infty} W_{\mathrm{A}}(\omega;\omega_0)(T_{\mathrm{gr}}(\omega) - \mu_{T\mathrm{gr}}(\omega_0))^2 d\omega, \quad (4)$$

where

$$W_{\mathrm{A}}(\omega;\omega_0) = W(\omega;\omega_0)\frac{A(\omega)}{\mu_{\mathrm{A}}(\omega)}, \quad (5)$$

$$S = \int_0^{\infty} W_{\mathrm{A}}(\omega;\omega_0)d\omega \quad \text{and} \quad \mu_{\mathrm{A}}(\omega_0) = \frac{\int_0^{\infty} W(\omega;\omega_0)A(\omega)d\omega}{\int_0^{\infty} W(\omega;\omega_0)d\omega} \quad (6)$$

The smoothing function used here is that of Konno and Ohmachi (1998):

$$W(\omega;\omega_0) = [\sin(\log_{10}(\omega/\omega_0)^b)/\log_{10}(\omega/\omega_0)^b]^4, \quad (7)$$

where b is an adjustable factor that controls the smoothing. The usual value $b = 20$ corresponds to a significant smoothing; a value $b = 40$ or $b = 60$ would imply a much smaller smoothing.

Figure 3d shows an example of group delay time $T_{\mathrm{gr}}(\omega)$ (dots) calculated from an observed acceleration motion recorded on the Volvi test site (Fig. 3a). The solid line corresponds to $\mu_{T\mathrm{gr}}(\omega)$, dashed lines to $\mu_{T\mathrm{gr}}(\omega) \pm \sigma_{T\mathrm{gr}}$. The amplitude spectrum $A(\omega)$ used in the calculation of group

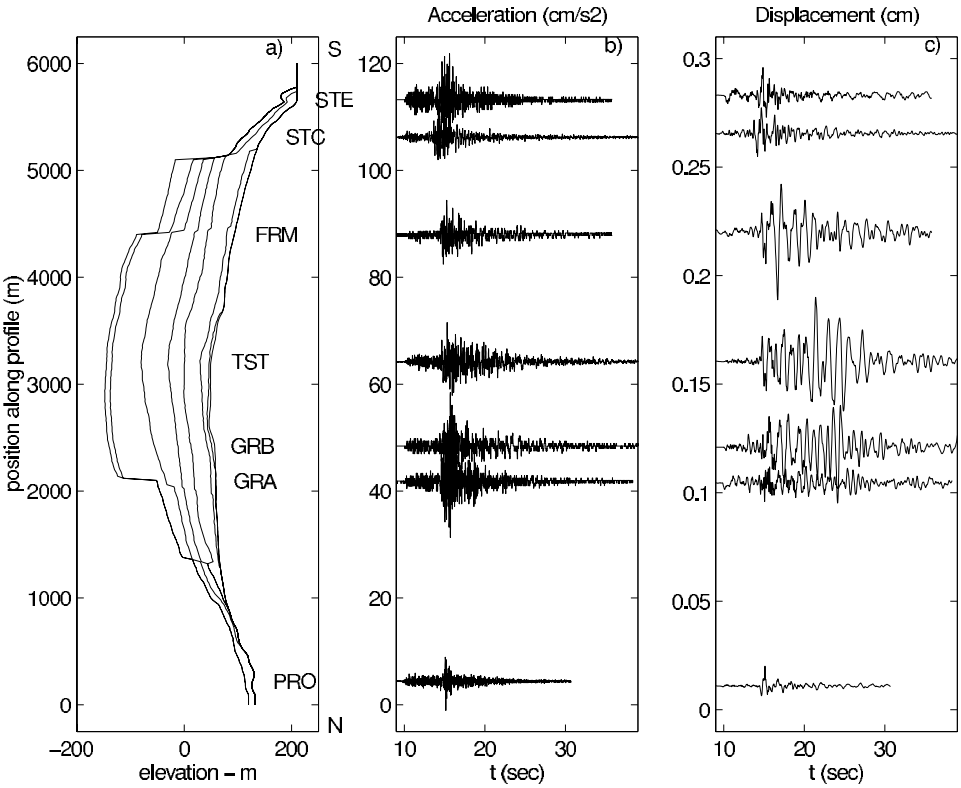

Figure 2. Observed acceleration and displacement motions of north–south components from a local event (04 April 1995 17:27) at permanent stations installed across the Volvi basin. The geophysical cross section shown was derived from geophysical and geotechnical data (Jongmans *et al.*, 1998).

delay time as well as the unwrapped phase are also presented (Fig. 3b, c). $\mu_{T\mathrm{gr}}(\omega)$ is therefore the mean arrival time of the wave group at frequency ω.

This method has been tested on a simple signal made of the summation of three truncated sinusoids with frequencies of 0.5, 1, and 5 Hz, and durations of 7, 2, and 3 sec, respectively (Fig. 4). It is inferred that the group delay is perfectly determined at the frequencies present in the signal: the 3.5-, 1-, and 1.5-sec values are respectively obtained at 0.5, 1, and 5 Hz. However, outside these frequencies, the calculated group delays have no significant meaning; it is therefore necessary to take the signal amplitude into account when applying the method. In addition, according to Sawada (1998), the previously defined variance is representative of signal duration for each frequency. The example displayed in Figure 4 clearly shows that $\sigma^2{}_{T\mathrm{gr}}$ is not linked to duration; variance only indicates the accuracy of $\mu_{T\mathrm{gr}}(\omega)$ estimation and is relatively small at 0.5, 1, and 5 Hz and large at other frequencies. This quantity will therefore not be used in the present study, and we claim it cannot be used as an estimate of the duration.

Estimation of Duration Lengthening

According to classical formalism, the signal recorded on surface $s^{\mathrm{O}}(t)$ is considered to be the convolution of source, path, and local effects:

$$s^{\mathrm{O}}(t) = s^{\mathrm{S}}(t) * s^{\mathrm{P}}(t) * s^{\mathrm{L}}(t) \tag{8}$$

where the superscripts O, S, P, and L stand for the observed signal, source, path, and local site effects, respectively. In the Fourier frequency domain, amplitude $A(\omega)$ and phase $\phi(\omega)$ spectra are therefore defined as follows:

$$A^{\mathrm{O}}(\omega) = A^{\mathrm{S}}(\omega) \cdot A^{\mathrm{P}}(\omega) \cdot A^{\mathrm{L}}(\omega) \tag{9}$$

$$\phi^{\mathrm{O}}(\omega) = \phi^{\mathrm{S}}(\omega) + \phi^{\mathrm{P}}(\omega) + \phi^{\mathrm{L}}(\omega). \tag{10}$$

By linearity,

$$T_{\mathrm{gr}}{}^{\mathrm{O}}(\omega) = T_{\mathrm{gr}}{}^{\mathrm{S}}(\omega) + T_{\mathrm{gr}}{}^{\mathrm{P}}(\omega) + T_{\mathrm{gr}}{}^{\mathrm{L}}(\omega) \tag{11}$$

and

$$\mu_{T\mathrm{gr}}{}^{\mathrm{O}}(\omega) = \mu_{T\mathrm{gr}}{}^{\mathrm{S}}(\omega) + \mu_{T\mathrm{gr}}{}^{\mathrm{P}}(\omega) + \mu_{T\mathrm{gr}}{}^{\mathrm{L}}(\omega) \tag{12}$$

We seek to determine $\mu_{T\mathrm{gr}}{}^{\mathrm{L}}(\omega)$, the group delay spectrum linked to the site effect (lengthening of the duration of seismic ground motions). A nearby reference site is used, $\mu_{T\mathrm{gr}}{}^{\mathrm{L}}(\omega)$ is estimated by subtracting the average group delay spectrum calculated from a recording at the analyzed station from the average group delay spectrum obtained from a recording of the same component at the reference site:

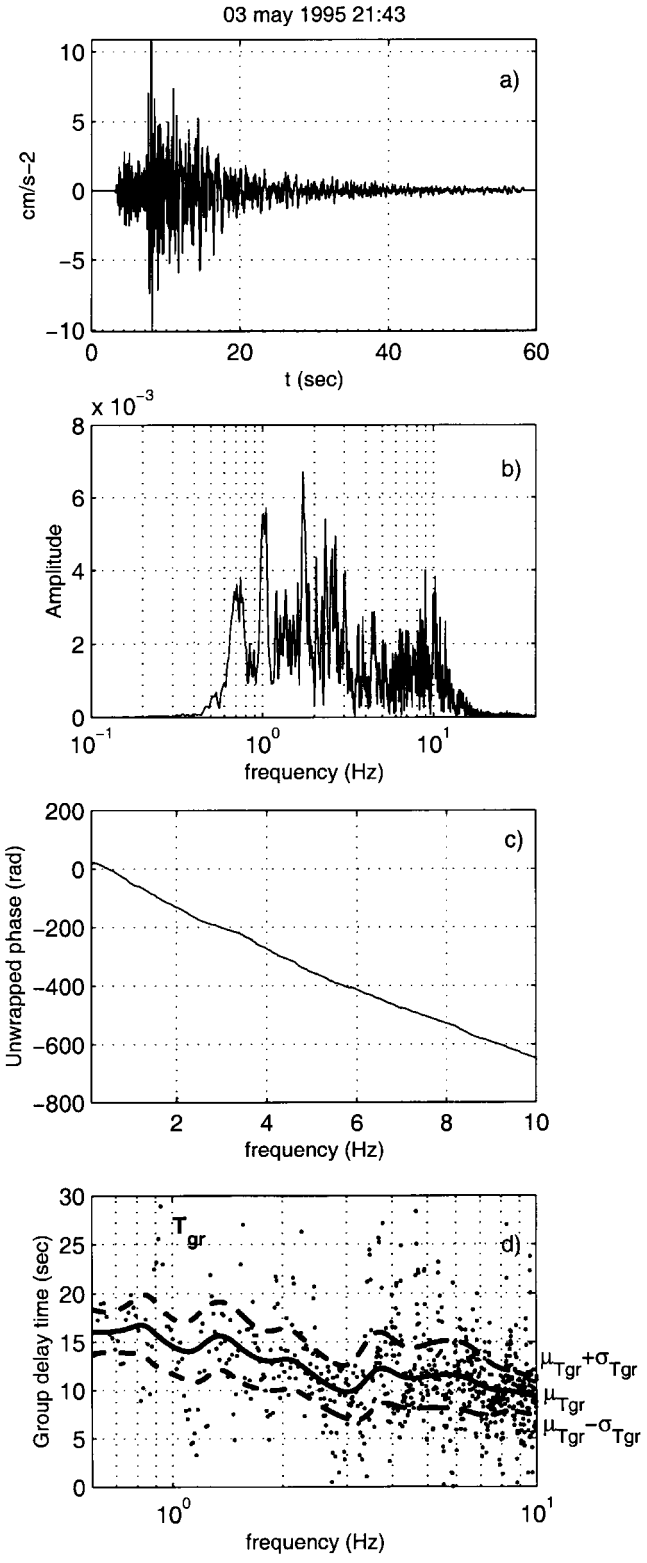

Figure 3. Example of group delay time calculated from an observed seismogram. (a) Acceleration motion observed at TST station in north–south component; (b) amplitude spectrum of observed ground motion that is taken into account in the smoothing of T_{gr}; (c) unwrapped phase spectrum, whose gradient is the group delay time T_{gr}; (d) dots, group delay time T_{gr} (ω) (sec); solid line, average spectrum of T_{gr} (ω), $\mu_{Tgr}(\omega)$; dashed lines, standard deviation $\sigma_{Tgr}(\omega)$.

$$\mu_{Tgr}{}^{L}(\omega) = \mu_{Tgr}{}^{O}(\omega)|_{\text{analyzed station}} - \mu_{Tgr}{}^{O}(\omega)|_{\text{reference site}}. \quad (13)$$

The reference site must be close enough to the analyzed station such that the source and path effects can be assumed equal at both stations. To be free of site amplifications and/or prolongations, it must be installed on outcropping hard rock without any topography. In principle, this method is analogous to the traditional spectral ratio method that estimates site amplification factors at different sites. In this case, the site response is determined by dividing the amplitude spectrum at the analyzed station by the amplitude spectrum at the reference site. When the previously described conditions are fulfilled, an estimate of $A^{L}(\omega)$ is thus obtained.

The quantity $\mu_{Tgr}{}^{L}$ will concern all results that follow. $\mu_{Tgr}{}^{L}(\omega)$ is the difference between two arrival times (at the analyzed station and at the reference) at frequency ω, so we will use interchangeably the terms "group delay spectrum" or "duration lengthening."

Results on Experimental Signals

Data

In this study we used two data sets recorded by the Euroseistest project. The first one corresponds to a swarm of events that occurred in the southeastern part of the Volvi lake in spring of 1995 (Table 1, magnitude range: $3.3 \leq M_L \leq 4.6$) (Raptakis *et al.*, 1998) Figure 1 shows the epicenters (stars) together with the observation sites. As in previous site amplification studies (Chavez-Garcia *et al.*, 2000; Raptakis *et al.*, 2000; Riepl *et al.*, 1998), these seven permanent stations are aligned on a cross section of the Volvi valley. Station PRO at the northern border (Fig. 2) is chosen as the reference station; STC and STE stations are located close to rock outcrops but are also close to a major normal fault. TST station is located in the center of the valley, at a site with about 200 m of sediments (soft at the very surface, but rather stiff at depths exceeding 50 m) (Jongmans *et al.*, 1998). Only three stations, PRO, STC, and TST had a 16-bit recording system at the time of the events. After examining the signal-to-noise (S/N) ratios of the records, we decided to consider the frequency range of 0.6–10 Hz. One of the records is shown in Figure 3. The seismograms are bandpass filtered between 0.6 and 40.0 Hz, and the whole signal available from the direct *P*-wave arrival is used in the calculation.

The second data set was obtained during the summer of 1994 when a temporary seismic network of more than 30 three-component stations was installed across the graben, with interstation distances of about 250 m (Riepl *et al.*, 1998) The present study is limited to the analysis of records obtained at seven of these stations that were connected to Reftek digitizers and broadband CMG40 sensors with an almost flat transfer function in the frequency domain down to about 0.05 Hz. Their location is the same as the permanent network. Records from seven local events are used with hy-

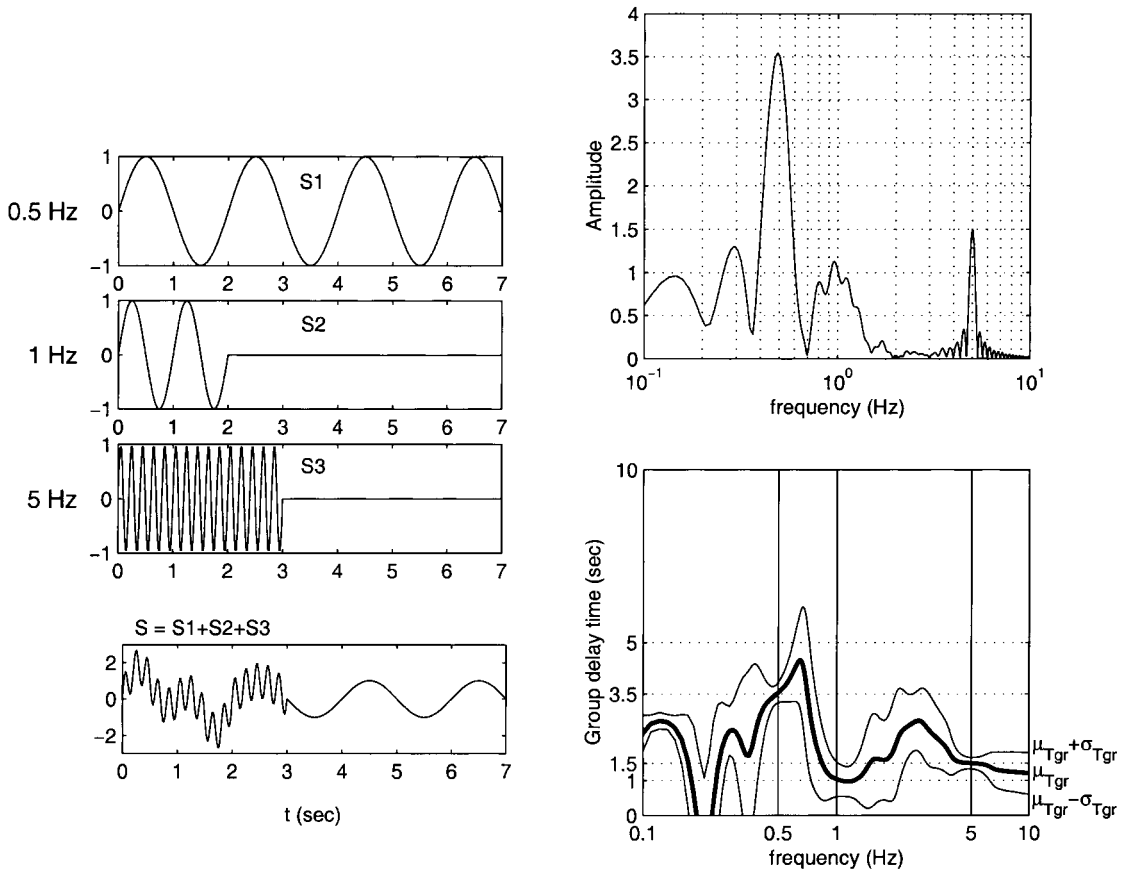

Figure 4. Test of the Sawada method (1998) on a simple signal made of the summation of three truncated sinusoids with frequencies of 0.5, 1, and 5 Hz and durations of 7, 2, and 3 sec, respectively. The amplitude spectrum is displayed. The thick line corresponds to group delay time $\mu_{Tgr}(w)$, thin lines show standard deviation.

Table 1
Moderate Earthquakes in Data Set 1

Date (yyyy/mm/dd)	Time	M_L	PRO	GRA	GRB	TST	FRM	STC	STE
1995/04/04	17:10	4.1	X	X	X	X	X	X	X
1995/04/04	17:27	3.8	X			X		X	
1995/05/03	14:16	3.9	X			X		X	
1995/05/03	15:40	4.2	X			X		X	
1995/05/03	18:56	3.8	X			X		X	
1995/05/03	21:36	4.5	X	X	X	X	X	X	X
1995/05/03	21:43	4.6	X	X	X	X	X	X	X
1995/05/03	22:33	4.3	X			X		X	
1995/05/04	00:43	3.6	X			X		X	
1995/05/04	01:14	3.3	X			X		X	
1995/05/07	09:26	3.5	X			X		X	

pocentral distances of less than 25 km and small magnitudes (Table 2, $M_L \leq 3$). The group delay is evaluated only at the values where the S/N ratio is greater than 3. The time series used begin with the *P*-wave arrival, but the coda is not always included because of the high noise level. The recorded signals at RFAR (FRM) station could not be used because of an excessive noise level.

Results and Discussions

Figure 5 displays results obtained for $\mu_{Tgr}{}^{L}$ at two representative sites: TST at the graben center and STE on the southern edge, for both north–south and east–west horizontal components, as well for the vertical component. The thick solid line corresponds to the mean values using all the available events, the averages being calculated by weighting the

Table 2
Weak Earthquakes in Data Set 2

Event	Date (yyyy/mm/dd)	Time	RPRO (PRO)	RROA	RGRE (GRA)	RTES (TST)	RFAR (FRM)	RTOW (STC)	RCHU (STE)
1	1994/06/24	05:48	X		X	X			X
2	1994/06/25	17:37	X		X	X			X
3	1994/07/02	22:49	X	X	X	X		X	X
4	1994/07/03	08:27	X	X	X	X		X	X
5	1994/07/04	10:55	X		X	X			X
6	1994/07/05	07:26	X	X	X				X
7	1994/07/05	21:02	X						X

group delay spectra by the normalized spectral content at the reference station:

$$\mu_{\text{mean}}(\omega) = \frac{\sum_{i=1,N} \mu_i(\omega) A_i(\omega)}{\sum_{i=1,N} A_i(\omega)}, \qquad (14)$$

where $\mu_{\text{mean}}(\omega)$ is the mean delay spectrum at frequency ω, $\mu_i(\omega)$ is the delay spectrum computed from event *i*, $A_i(\omega)$ the normalized spectral amplitude at the reference station (spectrum divided by maximum amplitude), and N is the number of event. One may notice a remarkable stability of group delay spectra, which highlights the reality of lengthening effect. Lengthening at STE station is approximately zero for the three components, as expected since the station is located very near to the bedrock on the southern border of the valley. On the other hand, TST station shows a rise in lengthening toward low frequencies with a maximum lengthening around 0.7–1.0 Hz, which corresponds exactly to the fundamental resonance frequency determined by various experimental means from weak events (Riepl, 1997). The observed trend on the north–south component is also found on the east–west and vertical components. Amplifications have also been calculated for the 11 analyzed events using PRO as the reference station (top of Fig. 5). Only the amplifications on the north–south component is shown on Figure 5, but similar trends are found on east–west and vertical components. The group delay spectra are stable from one magnitude range to the other: the average lengthenings obtained from events with magnitudes smaller than 3 show similar trends (Fig. 6). For TST station, a maximum prolongation of the signal duration is found around 0.7 Hz with identical values (5–6 sec). No lengthening is observed at STE station. The results show that the group delay method can be applied for a wide range of motion amplitudes.

The same study was performed for the recordings of the seven permanent strong-motion stations. Figure 7 shows the obtained results for $\mu_{T\text{gr}}^{\text{L}}$ on the north–south horizontal component at the six sites (except for the reference site) and for the 11 moderate magnitude events. Only three recordings are available at GRA, GRB, FRM, and STE stations because of the insufficient resolution level of the sensors. A structural cross-section of the basin is also presented, which allows linking the frequency of the lengthening peak to the alluvial thickness. The thicker the sediments, the lower the frequency at which the lengthening peak occurs. GRA and GRB stations show a maximum lengthening of signal duration between 1 and 2 Hz, whereas this peak occurs at 0.7 Hz at TST (site fundamental resonance frequency, Riepl *et al.*, 1998). Lengthening is small at STC and FRM sites; this is not surprising for STC, which is located near bedrock, on a thin sediment layer, as clearly observed in Figure 2. FRM, however, is placed above a thick alluvial layer. For these 11 events, waves come from the southeast. They are essentially diffracted on normal faults bordering the basin in the south and generate surface waves that propagate mainly from south to north. FRM is located above one of those faults inside the basin: surface waves are mixed with the arrival of direct *S* waves and so are barely visible on the site recordings. The surface waves are significant and appear clearly on the recordings of TST, GRA, and GRB stations; they propagate throughout the valley at a group velocity lower than direct *S*-wave velocity (300 to 400 m/sec) and arrive later. Ground-motion prolongation at the three stations is significant. The lengthening of signal duration really only occurs at low frequency, apparently due to the effects of anelastic attenuation.

Results on Synthetics Signals

Synthetics

The calculation of the group delay is applied to synthetic signals stemming from 2D numeric modeling based on the Volvi graben model presented in Figure 7 (Table 3) (finite-difference method, Moczo *et al.*, 1996; Chavez-Garcia *et al.*, 2000). We consider the surface response for six different incident impulses. Sources 1, 3, and 5 are Ricker wavelets with central frequencies of 1, 3, and 0.3 Hz; sources 7 to 9 are more realistic simulations, their time dependence is that of real signals recorded at the reference station PRO during three earthquakes (magnitudes 6.1, 5.3, and 2.0). In all the cases, excitations correspond to vertically incident plane waves (*SH* and *SV* for all cases). Excitations are specified on the lower border of the model. An example of synthetic signals, calculated every 300 m across the valley from source

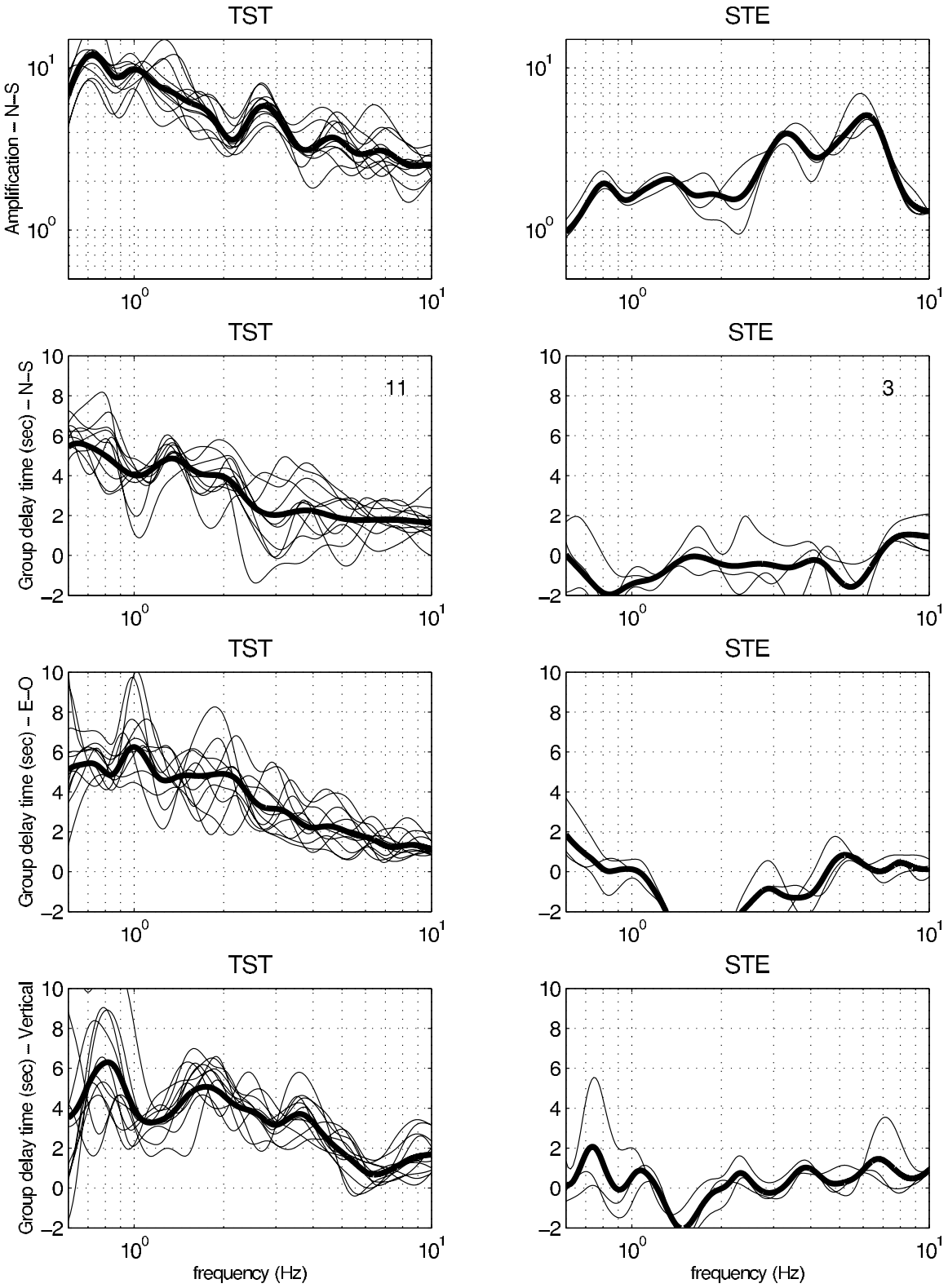

Figure 5. Amplification (north–south component) and group delay time of the three components evaluated at two stations: TST, which is in the center of the Volvi valley, and STE, which is on the southern border. Mean values are shown as a thick line on each figure. The used data set consisted of local moderate events (Fig. 1). Superimposed are the group delays corresponding to each event, and the number of records is indicated for each station. The reference station used is PRO.

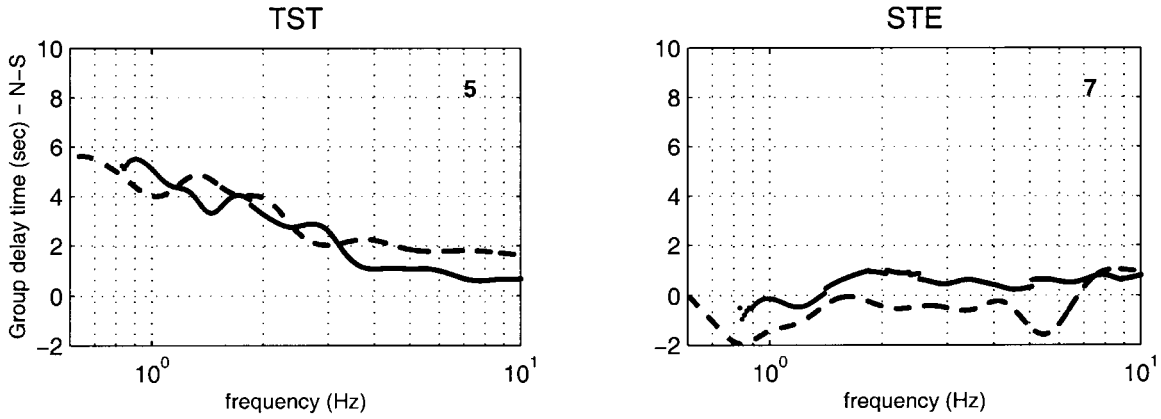

Figure 6. Comparison of mean group delays at two stations derived from recordings on the north–south component. The solid lines show the estimates obtained from weak events (the number of records used is indicated for each station), the group delays were evaluated only at the frequencies where the signal-to-noise ratio is greater than 3 and where at least three earthquakes were used in the computation. The dashed lines are the estimates obtained using the moderate events.

1, shows the important wave diffraction taking place on graben edges (Fig. 8).

First, group delays are determined from synthetic signals computed at the sites of the six permanent stations. Then, group delays are determined at 60 receivers placed every 100 m along the same profile, perpendicular to the valley axis. On each site the average is obtained by weighting the delay group values by signal spectral amplitudes at the reference station (normalized amplitudes with respect to maximum amplitude, see equation 14).

Results and Discussion

Results at the Locations of the Permanent Stations. The chosen reference station for the synthetics is, as for the observed signals, the PRO station located on the bedrock. The weighted average group delays are computed for the three components at the six permanent station sites. Synthetic results on longitudinal components are compared to observed mean delays (Fig. 9). We focus on frequencies where lengthenings occur. The frequency band where lengthenings occur for numerical synthetics coincides quite well with the real data. However, delays stemming from synthetic signals exhibit lower values, though the visual lengthening is very significant as may be observed on Figure 8 (source 1). At STC and STE, no duration lengthening is observed on the synthetics; the slight lengthening observed at STC for frequencies lower than 2 Hz is not found on synthetics. Lengthening in GRA and GRB synthetics occurs between 1 and 3 Hz, as it does for the real observations, although the real lengthenings are longer. The actual lengthening of signal duration at TST increases toward low frequencies, according to the observed mean curve. However, the frequency corresponding to maximum lengthening is slightly higher (1 Hz instead of 0.7 Hz). It is noted that lengthening at FRM is as significant as at TST, with a peak at 1 Hz. In the numerical computation, the input motion was specified as vertically incident *S* waves, whereas observations correspond to moderate events located southeast of the graben, with oblique incidence. This reinforces the hypothesis put forward earlier to interpret small lengthenings observed at FRM. For synthetics, vertical incidence leads to an important diffraction on both borders of the valley (south and north), and the prolongation is then significant at FRM.

Synthetic lengthenings are smaller than those observed experimentally. One explanation might be that quality factors allocated to the geophysical model (Table 3) may have been undervalued, causing waves to be attenuated more strongly than in reality and surface computed signal durations to be shorter. This difference in lengthening values is mainly noted at GRA and GRB stations: it could equally be due to the fact that, in the case of real events, surface waves are generated at the south border of the valley and their effects are thus greatest on the north side of graben. On the other hand, fault locations in the graben model on which synthetic signals are based may be uncertain.

Mean delays computed on the other two components (transverse and vertical) present similar features, and results are consistent with the experimental ones.

Results at 60 Receivers for the Three Components of Motion. The calculation of group delay was then applied to synthetic signals computed at 60 receivers located every 100 m across the valley. As previously, the reference station is located on a bedrock site outside the basin (receptor 1). A continuous representation of lengthenings according to frequency on the whole width of graben is displayed for the three components in Figures 10 and 11. On the horizontal components, maximum lengthening occurs at an increasingly low frequency from the borders to the center of the graben (0.7 Hz in the center), as expected. Amplifications were also computed from synthetic signals, and they are presented for the radial

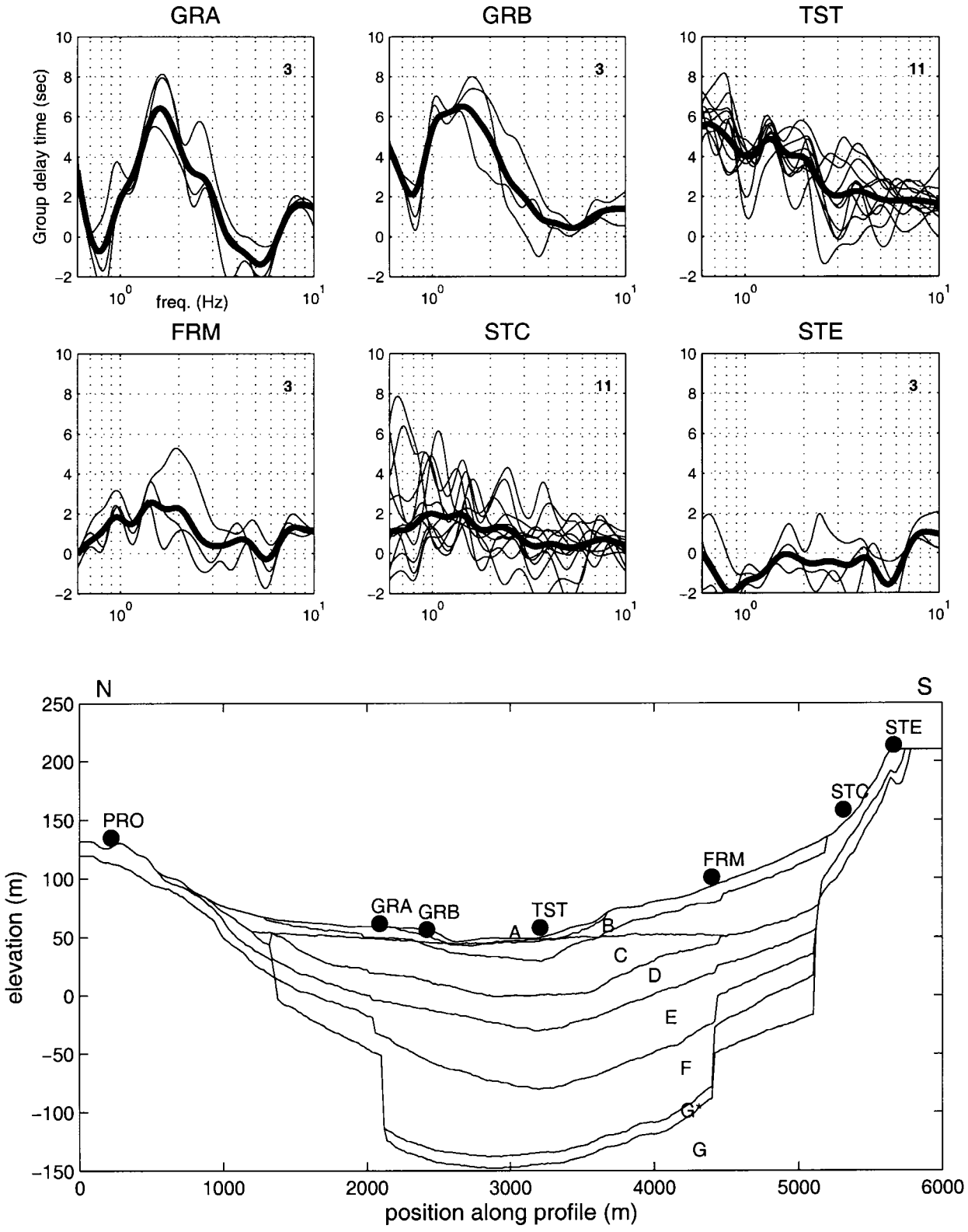

Figure 7. Mean lengthenings evaluated at the six permanent stations across the valley (thick line). The data set of moderate events was used; superimposed are the lengthenings corresponding to each event, the number of records is indicated for each station. The lower figure illustrates the location of these sites within the valley. See Table 3 for the description of the parameters allocated to each sediment layer of the geophysical model.

Table 3
Mechanical Characteristics of the Geophysical Model (Fig. 10)

Formation	A	B	C	D	E	F	G*	G
V_p(m/sec)	330	450	550	—	—	—	—	—
V_{pw}	—	1500	1600	2000	2500	2600	3500	4500
Q_p	90	45	70	60	120	150	150	250
V_s(m/sec)	130	200	300	450	650	900	1250	2600
Q_s	40	20	30	25	50	60	100	200
Gd (t/m3)	1.70	1.80	1.80	—	—	—	—	—
Gt (t/m3)	2.05	2.15	2.0	2.10	2.15	2.20	2.50	2.60

V_p, *P*-wave velocity; V_s, *S*-wave velocity; *Q*, Quality factor; $V_{pw} = V_p$ below water table; Gd/Gt, unsaturated/saturated density; G*, weathered rock.

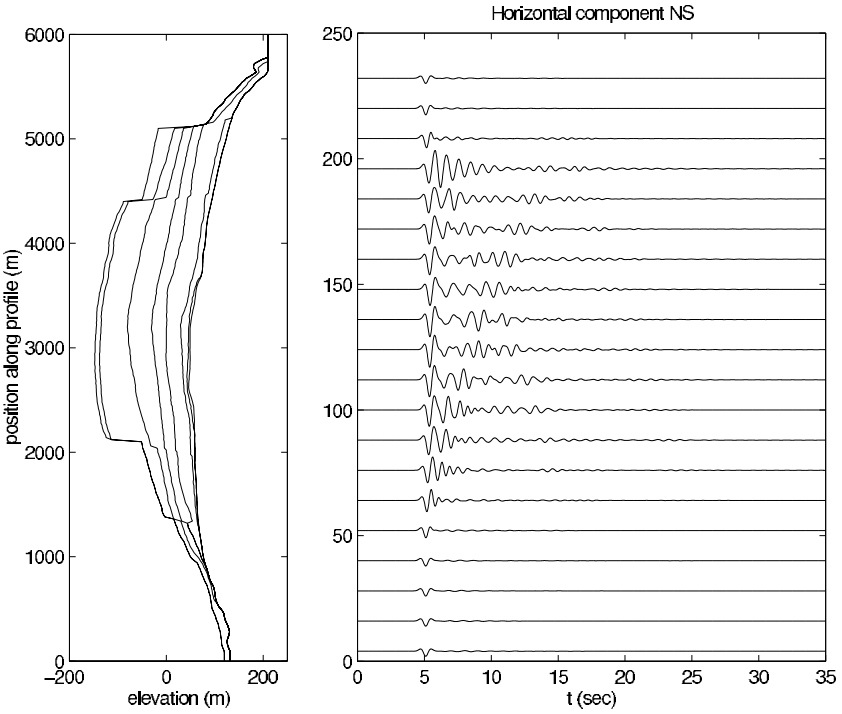

Figure 8. Synthetic signals stemming from 2D numeric modeling based on the Volvi graben model (source 1: Ricker wavelet with central frequency of 1 Hz). Signals are computed every 300 m across the valley.

component (Fig. 11). The thicker the sediment layer, the lower the frequency of fundamental resonance. Lengthenings remain significant up to 1.5 Hz in the central part of graben on the transverse component and up to 2.5 Hz on the radial component. At a higher frequency, they are no longer significant, in contrast with amplifications that remain at a high level up to about 5 Hz (Fig. 11): high frequencies are attenuated very quickly. Lengthenings begin at lower frequencies in the south of the basin than in the north, because the graben is asymmetric, elevations are higher and sediment layers are thicker in the south.

Lengthenings, which are nil beyond the faults edging the graben in the north and south, are increasingly high from the borders to the center of valley. A sharp change is noted across the fault separating geological units from the bedrock in the south (receptor 51 to 52): this interface slope is indeed very steep. No sharp change is observed on the north border, where alluvial thickness variations are smoother. Maximum values obtained on both horizontal components have the same size range but are slightly higher on the transverse component. This is due to the fact that the phase and group velocities are lower for Love waves than for Rayleigh waves.

Results on the vertical component show different features from those of the horizontal ones. Lengthening of peaks occurs at higher frequencies (1.5 Hz in the graben center), and lengthening remains at a significant level on a wider frequency range (between 1.5 and 3.5 Hz). The differences between horizontal and vertical components have already been highlighted in the case of amplifications (Riepl *et al.*, 1998). Lengthenings reach higher values than for horizontal components (6 sec vs 4.5 sec maximum horizontally) and remain concentrated in the middle of graben where sediment layers are thickest. Furthermore, clear changes are observed across normal faults in the south (receptors 44 to 45 then 49 to 50). The high values present at very low frequency and up to 3 Hz on the north border are certainly numerical

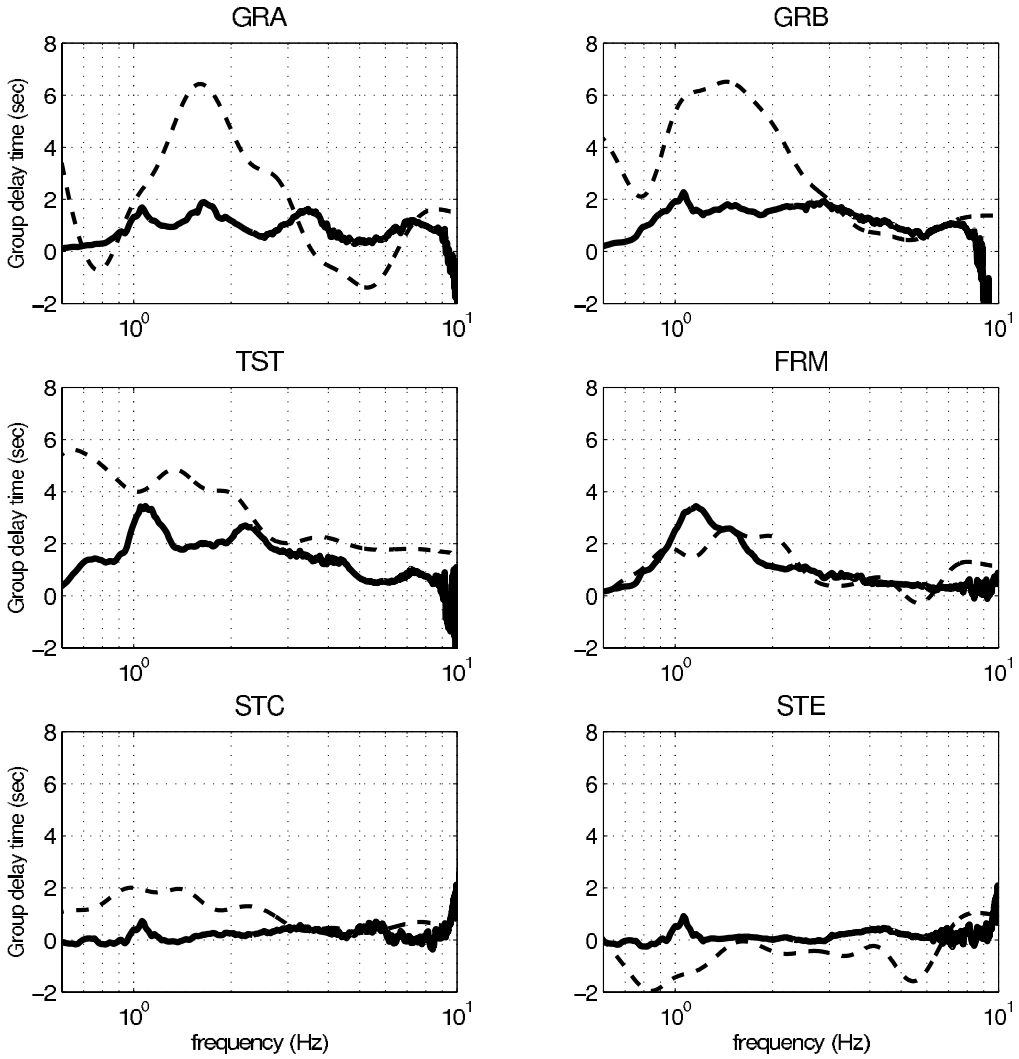

Figure 9. Comparison between the synthetic lengthenings (solid lines) and those observed (dashed lines) in the north–south component at the sites of the six permanent stations.

artefacts. Their origin is probably linked to the very low energy on vertical component at these frequencies and locations and therefore to the lack of precision of group delay estimates.

The sharp velocity contrasts between the bedrock and basin sediments refract upcoming waves to near vertical incidence. We therefore attribute movements on the horizontal components primarily to *S* waves and those on vertical components to *P* waves. Moreover, *P*-wave velocities are higher than those of *S* wave. Consequently, if the fundamental resonance frequency is grossly considered to be equal to $c/4h$ (where h is the thickness of sediments and c is the wave velocities), the fundamental resonance frequency obtained is higher on the vertical component than on the horizontal, as shown by observations.

Significant lengthenings present between 1.5 and 3 Hz on vertical and radial components and absent on transverse components are probably linked to Rayleigh waves generated on the borders of graben (interactions between *P* waves and *SV* waves). Lengthenings on both vertical and radial components are significant over a wider frequency range than they are on the transverse component, probably corresponding to the fact that *P* waves (and therefore Rayleigh waves) are less attenuated than *S* waves (and therefore Love waves).

Application: Synthetic Signals Computation

This technique provides information on the effects of site conditions on the ground-motion phase and hence on the time domain distribution of energy. We have therefore tested its use for reconstructing realistic, site-specific synthetic signals. The basic idea is to derive a complex transfer function accounting for both the modulus amplification and the phase changes and to convolve it with the prescribed signal on reference rock.

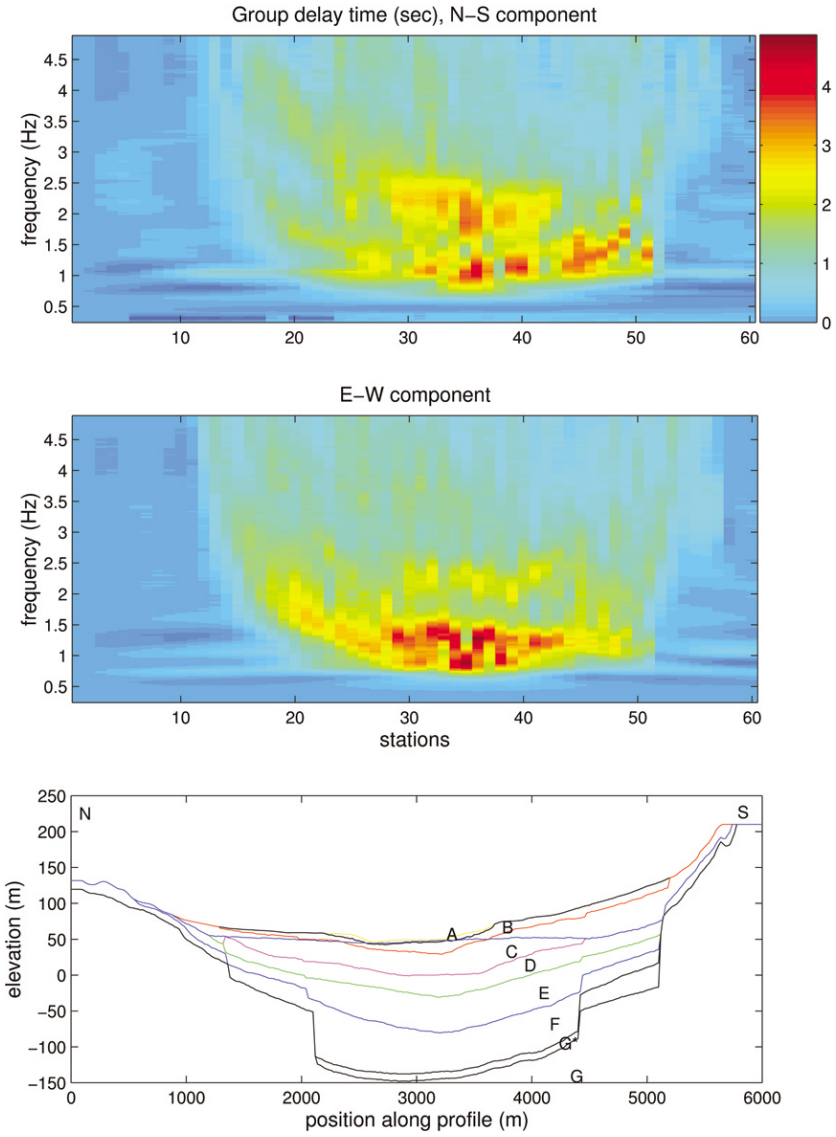

Figure 10. Synthetic mean group delays of horizontal components evaluated at stations across the valley (from north to south). See Table 3 for the description of the parameters allocated to each sediment layer of the geophysical model.

The procedure may be described as follows:

1. Select a signal *r(t)* for the reference site on rock
2. Compute its Fourier spectrum $R(\omega) = B(\omega) \exp(-i\varphi_R(\omega))$, where $B(\omega)$ is the modulus and $\varphi_R(\omega)$ is the phase
3. Modify the modulus of the rock motion according to the observed amplification derived from the soil site to rock spectral ratio $SR(\omega)$ and get a new Fourier modulus $A(\omega) = B(\omega) \cdot SR(\omega)$
4. Modify the phase according to the observed group delay

$$\varphi_L(\omega) = \varphi_R(\omega) + \int_0^{\omega} \mu_{Tgr}{}^L d\theta \qquad (15)$$

5. Build a new complex Fourier spectrum $S(\omega) = A(\omega) \exp(-i\,\varphi_L(\omega))$
6. Reconstruct a time domain synthetics $s(t)$ by taking the inverse Fourier transform of $S(\omega)$

As an example, this simple method has been applied at site TST with the recording at reference station PRO corresponding to the 3 May 1995 14:16 event (Table 1). Lengthening was computed between 0.5 and 10 Hz from the group delays derived from the three moderate events with largest S/N ratios. The synthetic phase therefore equals the reference phase at frequencies under 0.5 Hz and beyond 10 Hz. Figure 12 displays the recorded signal at station TST (Fig. 12a), together with the reference seismogram (Fig. 12b) used to compute the synthetic signal (Fig. 12c). The three seismograms are also shown after a low-pass filtering under 2 Hz. One may clearly identify the lengthening of the reconstructed signal, especially on the low-pass-filtered series because the lengthening is maximum around 1 Hz. Of course, there is not a perfect matching between the actual recordings

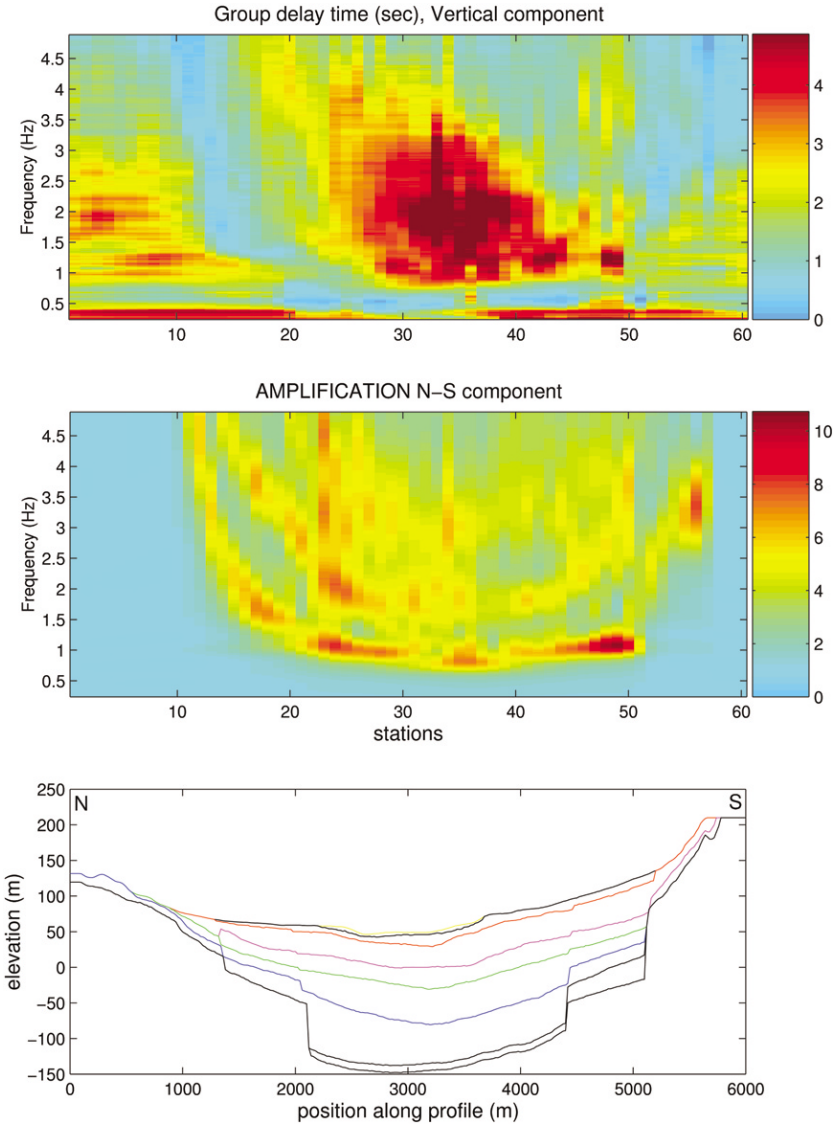

Figure 11. Synthetic mean group delays of vertical component and synthetic mean amplifications of radial (north–south) component evaluated at stations across the valley (from north to south).

and the reconstructed signals, but the overall resemblance is very satisfactory.

As the phase changes were found to be comparable for weak and moderate events, one may consider applying this technique to expected strong motions on the basis of complex Fourier transfer functions derived from weak events. Two obvious shortcomings need to be kept in mind: (1) a good S/N ratio is required to derive a robust estimate of the mean group delay; and (2) unless the phase and amplitude changes are measured on strong-motion records, this method cannot account for nonlinear effects.

However, we do think this technique is very promising and should be tested at many different sites.

Conclusion

This study has successfully tested an improved method for the measurement of site effects and proposes a new technique for reconstructing site-specific time domain signals. The method is an extension of the classical spectral ratio method to include not only modulus but also phase changes. The phase modifications are obtained using the mean group delay technique proposed by Sawada (1998), which basically measures, for each frequency, the central arrival time of the wavelet, derived from the frequency derivative of the unwrapped phase. Comparing the mean group delay on a reference site and on the site under study, we can infer site-specific modifications that are interpreted as changes in signal duration related to site geology. Although the group delay does bear some relation with the (frequency-dependent) signal duration, this relation is not simple. For instance, if we assume that energy is distributed in the time domain with a boxcar window, the total duration is simply twice the group delay. In real signals, however, the time domain envelope is usually far from a boxcar, and the actual duration is therefore probably significantly larger than simply twice the mean group delay. We tested the Sawada (1998) claim that signal duration could be accurately derived from the variance of

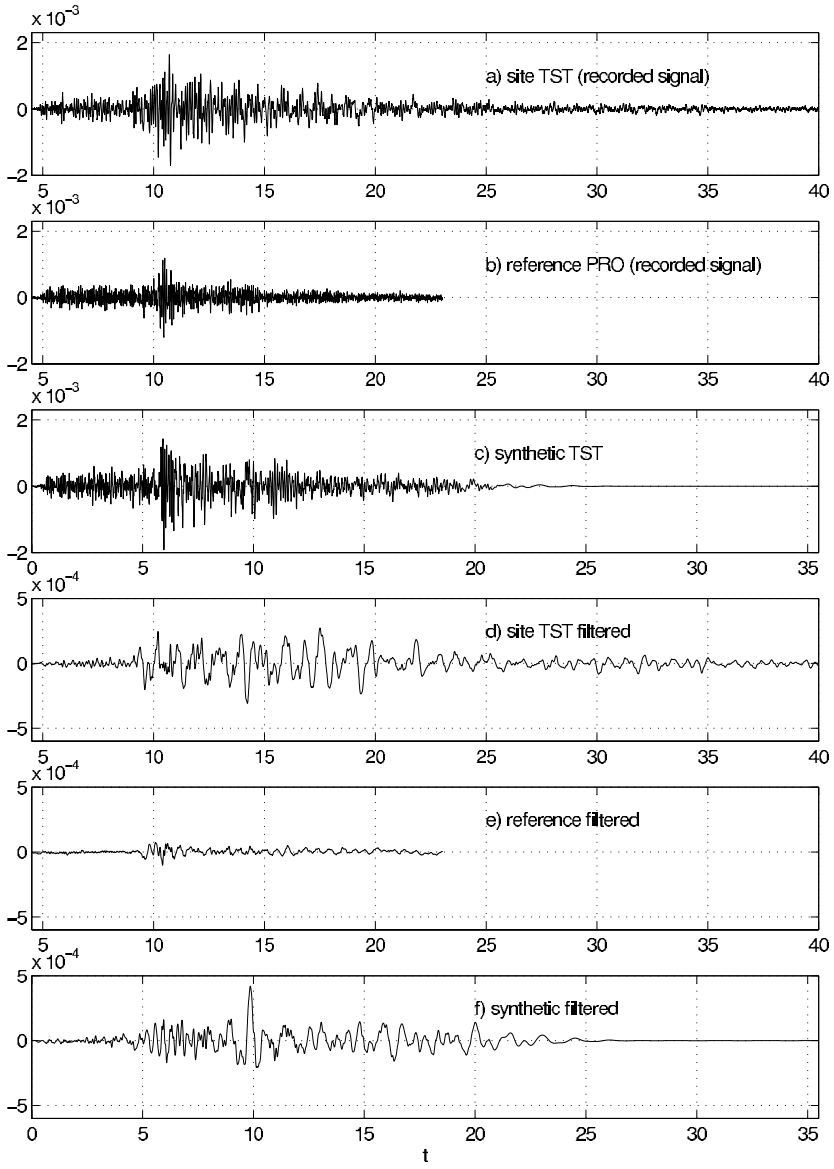

Figure 12. Synthetic signal computed at site TST (c) using the seismogram recorded at reference station PRO (b), compared to the real seismogram recorded at station TST (a). The three following signals are the same as above after a lowpass filter under 2 Hz.

mean group delay estimates: our tests indicate that this quantity only indicates the accuracy of the mean group delay calculation. We therefore focused, in the present study, on the differences in the mean group delay spectra between sites under study and the reference site.

We then applied this technique to weak and moderate motion recordings obtained in the Volvi test site graben structure.

1. The first important result is that the experimental group delay spectra exhibit a rather satisfactory stability, though evaluated from events of varied magnitudes ($2.5 < M_L \leq 4.6$) and variable epicentral distances and azimuths. Their estimation are quite sensitive to S/N ratio levels: a minimum threshold value of 5 is recommended.
2. The second result is that the increase of group delay appears closely related to the local geology (in Volvi, an active graben filled with recent deposits) and the amplification pattern. The maximum increase almost systematically occurs at each site's fundamental resonance frequency, whereas at higher frequencies, the ground-motion prolongation is no longer significant, even though there still exist some modulus amplification.
3. The third result concerns the amount of group delay increase: in the Volvi case, we measured differences up to a few seconds around 1 Hz in the center of the graben. These values may look rather low. However, one must keep in mind the actual signal lengthening is significantly larger.

These observations were then compared with results of a similar processing on synthetic signals obtained with a finite-difference modeling of the seismic response of the graben to incident *SV* and *SH* plane waves. This comparison yielded a very satisfactory qualitative consistency: the frequency ranges where significant lengthenings occur are

similar. However, the group delays derived from synthetics are systematically smaller than observed in real data (2 sec versus 4–6 sec). It may indicate that some of the mechanical parameters selected for the basin model in the 2D computations (see Jongmans *et al.*, 1998) should be modified. For instance, higher quality factors would induce longer durations due to lower damping of local surface waves. It also suggests that this technique might be a very promising tool to discriminate the respective importance of 1D and 2D or 3D effects at a given site: the former, related with up and down bouncing and short travel times, would produce only very small duration increase, whereas the latter would involve lateral propagation and reverberations, with much larger travel times, and produce large duration increases.

Finally, we proposed a new technique to reconstruct site-specific time domain synthetics. This technique was illustrated on a single example from the Volvi test site, where it does allow retrieval of the nonstationary time domain changes with larger duration increase at lower frequencies. As the response of nonlinear structures (including soil structures) is highly sensitive to the time domain distribution of incoming energy, this technique might prove useful in generating realistic synthetics compatible both with regulatory spectra and the actual physics of site effects.

Frequency domain amplitudes have been until now extensively used for site response investigation, but so far, phase has received less attention. Analysis of group delay is a new tool that can be used to describe the phase of real signals and thus check the validity of the phase of synthetic signals. Given the stability of group delay differences, we recommend that this simple method of seismic-motion prolongation estimation be systematically applied in all instrumental site effect studies. We must, however, stress the fact that it is essential to use local event records with an excellent S/N ratio in order to obtain stable results, since estimation of the phase is very sensitive to ambient noise. Keeping this limitation in mind, we are rather optimistic as to the applications of this technique, both for an improved understanding of actual site effects at real sites and for improving the way they are practically taken into account in engineering projects.

Acknowledgments

This study was supported by the European Commission through the Grants ERBIC15 CT96-0210, ENV4-CT96-0255, and ERBIC15 CT96-0210. Special thanks are due to the ITSAK and Aristotle University teams for installing and maintaining the strong-motion instruments. We gratefully thank two anonymous reviewers, whose comments greatly improved the manuscript.

References

Bard, P.-Y., J. Kristek, P. Moczo, J. Riepl-Thomas, (1999). Finite-difference modeling of site effects in the Grenoble basin, in *Abstracts of IUGG 99*, Birmingham, England, 26–30 July 1999.

Chavez-Garcia, F. J., D. Raptakis, K. Makra, and K. Pitilakis, (2000). Site effects at Euroseistest. II. Results from 2D numerical modeling and comparison with observations, *Soil Dyn. Earthquake Eng.* **19,** no. 1, 23–40.

Jongmans, D., K. Pitilakis, D. Demanet, D. Raptakis, J. Riepl, C. Horrent, G. Tsokas, K. Lontzetidis, and P.-Y. Bard (1998). EURO-SEISTEST: determination of the geological structure of the Volvi basin and validation of the basin response, *Bull. Seism. Soc. Am.* **88,** no. 2, 473–487.

Konno, K., and T. Omachi (1998). Ground-motion characteristics estimated from spectral ratio between horizontal and vertical components of microtremor, *Bull. Seism. Soc. Am.* **88,** no. 1, 228–241.

Moczo, P., P. Labak, J. Kristek, and F. Hron (1996). Amplification and differential motion due to an antiplane 2D resonance in the sediment valleys embedded in a layer over the halfspace, *Bull. Seism. Soc. Am.* **86,** 1434–1446.

Raptakis, D., F. J. Chavez-Garcia, K. Makra, and K. Pitilakis (2000). Site effects at Euroseistest. I. Determination of the valley structure and confrontation of observations with 1D analysis, *Soil Dyn. Earthquake Eng.* **19,** no. 1, 1–22.

Raptakis, D., N. Theodulidis, and K. Pitilakis (1998). Data analysis of the Euroseistest strong motion array in Volvi (Greece): standard and horizontal to vertical ratio techniques, *Earthquake Spectra* **14,** no. 1, 203–224.

Riepl, J. (1997). Effects de site: évaluation expérimentale et modélisations multidimensionnelles, application au site test EURO-SEISTEST (Grèce), *Thèse de Doctorat*, Université Joseph Fourier, Grenoble I, 227 pp. (in French).

Riepl, J., P.-Y. Bard, D. Hatzfeld, C. Papaioannou, and S. Nechtschein, (1998). Detailed evaluation of site response estimation methods across and along the sedimentary valley of Volvi (EURO-SEISTEST), *Bull. Seism. Soc. Am.* **88,** no. 2, 488–502.

Sawada, S. (1998). Phase characteristics on site amplification of layered ground with irregular interface, in *The Effects of Surface Geology on Seismic Motion*, K. Irikura, K. Kudo, H. Okada, and T. Sasatani (Editors), Balkema, Rotterdam, 1009–1013.

Laboratoire de Géophysique Interne et Tectonophysique
Maison des Geosciences
BP 53 38041
Grenoble Cedex 9, France
(C.B., P.Y.B.)

Institut de Radioprotection et de Sûreté Nucléaire
SERGD/BERSSIN
BP 17-92262
Fontenay-aux-Roses Cedex, France
(C.B.)

Laboratoire Central des Ponts-et-Chaussées
58, bd Lefebvre
75732 Paris Cedex 15, France
(P.Y.B.)

Geophysical Institute
Slovak Academy of Sciences
Dubravska cesta 9
845 28 Bratislava, Slovak Republic
(P.M., J.K.)

Manuscript received 12 October 2001.